FINAL PROGESS REPORT

Image Guided Constitutive Modeling of the Brain Tissue

PI: Oskar Skrinjar, Department of Biomedical Engineering
Georgia Institute of Technology

Summary:

The following is an aim-by-aim summary of the project "Image Guided Constitutive Modeling of the Brain Tissue". The details are explained in [1], which is attached to this report. The used research materials, data, and software are not directly available to other investigators but are explained in the publications.

Aim 1: Physical modeling of the behavior of brain with tumor using phantom of the left hemisphere of human brain cast from silicon gel and subjected to "ventriculostomy" and "indentation" tests.

Summary 1: We have developed deformable physical phantoms of a human brain hemisphere. The phantoms were constructed of a silicon gel because it has similar mechanical properties as the brain soft tissues. The phantoms contained a cavity simulating a lateral ventricle. The entire set-up allowed for the control of the pressure outside the phantom and inside the cavity.

Aim 2: Image based derivation of the strain fields from pre- and post-deformation CT images of the brain phantom.

Summary 2: We acquire CT images of the deformable phantom at different stages of the applied deformation. To obtain the deformation of the phantom from the pre- to post-deformation CT image, we registered the images. This process has two steps: rigid registration (to remove rotation and translation between the two images) and non-rigid registration (to compute the displacements between the rigidly registered pre- and post-deformation images).

Aim 3: Inverse finite element analysis of the strain fields and derivation of constitutive models within the novel thermodynamically consistent framework – Hyperplasticity.

Summary 3: Once the deformation from the pre- to post-deformation CT image was obtained (Aim 2), we segmented the phantom in the pre-deformation CT image, constructed an FEM mesh, and used a Levenberg-Marquardt based inverse analysis algorithm to compute the mechanical model parameters. We used the neo-Hookean and Ogden models.

Aim 4: Verification of the numerical models against the data from the element tests on the samples extracted from the "healthy" tissue and the "tumor", after the latter is removed from the phantom.

Summary 4: The calculated mechanical properties were consistent with those in the literature and those obtained from the independent uniaxial compression tests, providing preliminary justification for the future application of the Image Guided Constitutive Modeling to in-vivo brain tissue, which has a number of clinical applications.

Significant Results:

We were able to achieve the goal of the project: to develop and test concepts of Image Guided Constitutive Modeling (derivation of mechanical properties of an object from pre- and post-deformation images) on deformable brain phantoms.

Publications:

1. Puzrin, A., Ozan, C., Germanovich, L., Mukundan, S., Skrinjar, O., "Inverse 3D FE Analysis of a Brain Surgery Simulation", *Computational Biomechanics for Medicine*, Copenhagen, Denmark, October 2006.
   NOTE: - this is a full (10-page) paper
   - CBM is a peer-reviewed conference

2. Puzrin, A., Skrinjar, O., Ozan, C., Kim, S., Mukundan, S., "Image Guided Constitutive Modeling of the Silicone Brain Phantom", *SPIE Medical Imaging*, San Diego, CA, USA, February 2005.
   NOTE: this is a full (8-page) paper

3. Skrinjar, O. and Tagare, H., "Symmetric, Transitive, Geometric Deformation and Intensity Variation Invariant Nonrigid Image Registration", *IEEE International Symposium on Biomedical Imaging*, Proceedings, Arlington, VA, USA, April 2004.
   NOTE: - this is a 4-page paper
   - ISBI is a peer-reviewed conference

Human subjects:

The project did not involve any human subjects.

Inverse 3D FE Analysis of a Brain Surgery Simulation

Alexander Puzrin[1], Cem Ozan[2], Leonid N. Germanovich[2], Srinivasan Mukundan[3], and Oskar Škrinjar[4]

[1]ETH Zurich, Inst. for Geotechnical Engineering., Zurich, Switzerland
[2]Dept. of Civil and Environmental Engineering, Georgia Tech, Atlanta, GA, USA
[3]Dept. of Radiology, Neuroradiology, Duke Univ. Medical Center, Durham, NC, USA
[4]Dept. of Biomedical Engineering, Georgia Tech, Atlanta, GA, USA
oskar.skrinjar@bme.gatech.edu

Abstract. Image Guided Constitutive Modeling (IGCM) is a novel approach to development of reliable constitutive models of the mechanical behavior of the in-vivo human brain tissue. We propose to take the MR or CT scan of a brain response to ventriculostomy. Image-derived displacement fields are then used by 3D inverse analysis to develop the constitutive models of the brain tissue. In this paper, the IGCM is demonstrated on the silicone brain phantoms closely simulating the in-vivo brain geometry, mechanical properties and boundary conditions. The ventriculostomy was simulated by consequently inflating and deflating the internal rubber membrane. The obtained images were analyzed to derive displacement fields, which was followed by Inverse Finite Element Analysis to obtain the parameters of the neo-Hookean and Ogden elastic models for the phantom material. The calculated mechanical properties were consistent with those in the literature and those obtained from the independent uniaxial compression tests, providing preliminary justification for the future application of the IGCM to in-vivo brain tissue.

Key words: constitutive modeling, silicon brain phantom, nonrigid image registration, 3D inverse analysis

1 Introduction

Augmentation of accuracy of image-guided neuroprocedures can be achieved by modeling intra-operative brain deformations using the numerical and analytical tools of the Mechanics of Continuum Media. This approach requires reliable constitutive models of the mechanical behavior of in-vivo human brain tissues. The main obstacle in the development of reliable constitutive models of the brain tissues is that the standard element tests (i.e. uniaxial compression/extension and pure shear) are not feasible in-vivo, while the ex-vivo mechanical properties of the tissue may be quite different. We propose to define the mechanical properties of the brain tissue in-vivo by taking the global MR or CT images of a brain response to ventriculostomy - the relief of the elevated intracranial

pressure (ICP). Using state-of-the-art 3D image analysis, these images can be translated into displacement and strain fields. Using inverse analysis of the brain response, the constitutive models of the brain tissue can be developed.

This inverse analysis represents a challenging coupled imaging-mechanical problem, which we will term Image Guided Constitutive Modeling (IGCM). The IGCM is a complex iterative process of adapting a chosen constitutive model to mimic the deformed tissue behavior. It can be briefly described as follows. A Finite Element code utilizes an adopted model to solve the boundary value problem simulating the ventriculostomy. The predicted displacement field is then compared to the measured one and the model is modified to ensure the best fit between the two fields.

Puzrin et al. [1] provided the preliminary 2D demonstration how the concepts of the Image Guided Constitutive Modeling function in the controlled environment: on the brain phantoms, with the approximate simulation of the in-vivo brain geometry, mechanical properties and boundary conditions. The purpose of this paper is to extend the IGCM application to the 3D inverse analysis of the new experimental simulation of ventriculostomy with improved initial and boundary conditions.

2 Mechanical Behavior of the Brain Tissue

The first issue to be resolved in this work was the choice of the model material. Its mechanical behavior should be similar to that of the live brain tissues. Mechanical properties of living tissues, in particular, of muscular-skeletal system, skin, lungs, blood and blood vessels have attracted much attention in the Biomechanics [2]. The properties of very soft tissues (brain, liver, breast, etc.), which do not bear mechanical loads, have not been studied with the same rigor.

The early continuum mechanics constitutive models utilized in brain tissue analysis were linearly elastic or visco-elastic [3, 4]. Pamidi and Advani [5] employed the strain energy function proposed by Mooney [6] leading to a non-linear viscoelastic model.

It is generally accepted that the intracranial pressure-volume relationship is determined by mechanical properties of the brain tissues. In order to describe these properties for the intracranial pressure test interpretations, Walsh and Schettini [7] proposed a two parameter logarithmic relationship between the depth of the pressure transducer insertion and the measured pressure. Sahay et al. [8] used the elastic strain energy potential proposed by Hart-Smith [9] for rubber materials, resulting in a non-linear hyperelastic constitutive model. Viscous effects in the above models were neglected.

To model constitutive behavior on animal brain, recent works [10, 11] used a well known Mooney-Rivlin type energy function, originally developed for incompressible rubbers [12]. It appeared, however, that this function cannot account for a different behavior in extension than in compression, exhibited by brain tissue [13], and it was suggested to utilize the Ogden energy function instead, which had been also originally proposed for incompressible rubbers [14].

3 Preparation of the Brain Phantoms

A relative success of the incompressible rubber constitutive models in describing mechanical behavior of the animal brain suggests that rubbers can be used as a physical model material to simulate mechanical behavior of human brain tissue. Physical brain phantoms made of rubber materials have been used both for head injury analysis and in experiments simulating applications in neurosugery. Bradshaw et al. [15] and Ivarsson et al. [16] used a silicone gel brain model to analyze the effect of a head impact on brain injury. Audette et al. [17] used a brain phantom made of Polyvinyl Alcohol Cryogel to simulate the brain shift problem. Brands et al. [18], have shown that Dow Corning Sylgard 527 Dielectric Silicon Gel [19] mimics closely the viscoelastic brain tissue properties at low frequency quasi-static loads. Azar et al. [20] showed that its mechanical behavior is well described by the Mooney-Rivlin model [12]. Rajagopal et al. [21] showed that Silicone gel could be modeled by neo-Hookean [22] material law.

In this work, a plastic mold (Fig. 1a)- about 23 x 18 x 11 mm - of the left hemisphere of human brain was used to cast the brain phantom (Fig. 1b) using Dow Corning Sylgard 527 Dielectric Silicon Gel [19]. This silicone gel system is composed of 2 parts, catalyst and resin, that are mixed to prepare the gel. In our experiment, catalyst and resin were mixed in the ratio of 1:1. While curing the silicone gel in the mold, a plastic pipe of 2 cm diameter circular cross section was placed at the center of the mold. Sample was cured in 55^oC for 16 hours. After the curing, the pipe was removed and a rubber membrane was placed inside the hole to model the lateral ventricle. One millimeter diameter "bubbles," made by mixing silicone grease with graphite powder, were injected into the phantom in a regular 3D grid of about $1.5 \times 1.5 \times 1.5$ cm^3 in order to enable detection of the displacement field in the CT images.

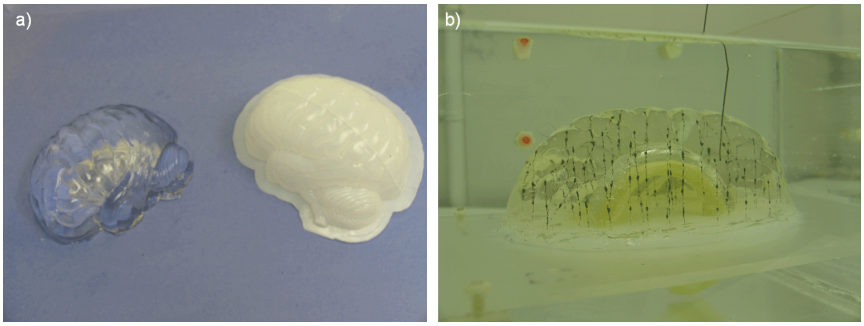

Fig. 1. (a) Plastic mold. (b) Brain phantom.

4 Experimental Program

The clinical procedure simulated in the experiments is called ventriculostomy (or "shunting") - the relief of the elevated intracranial pressure (ICP). It is used to treat the non-communicating hydrocephalus, a medical condition manifesting itself in obstructed flow of the cerebral spinal fluid (CSF) from the lateral ventricles into the subarachnoid space. This procedure has a number of important advantages for the Image Guided Constitutive Modeling. First of all, it is very common - a large hospital (e.g. Duke, Emory) performs several hundreds of ventriculostomies per year (Mukundan, private communication). The ICP during the procedure can be easily monitored. CT scans are regularly taken before and after the procedure, providing the brain configuration at the two known levels of the ICP. The change in the boundary conditions involves entire brain - not just its part. And, finally, the boundary conditions are very simple - they are given by a change in the hydrostatic pressure.

The experimental setup (Fig. 2a) was designed to model both communicating and non-communicating "hydrocephalus" with subsequent "ventriculostomies" by independently controlling the outer and inner pressures in the phantom. No metal parts were used in the setup construction allowing for the experiments to be conducted in both CT and MR environments. The setup consists of a hermetic transparent Plexiglas cell with a pedestal, to which the phantom is fixed with silicone sealant, and two standpipes allowing for independent pressure/volume control both in the cell and in the ventricle. The available pressure range is 0 - 5 kPa with resolution of 0.01 kPa, which is consistent with the range of both normal and abnormal CSF pressures.

The experiments were carried out at Emory University Hospital in General Electric LightSpeed 16 Computed Tomography scanner (Fig. 2b). The non-communicative hydrocephalus and ventriculostomy were simulated as illustrated in Fig. 3. First, same magnitude of hydrostatic pressure was applied on both inner and outer surfaces of the phantom (intermediate configuration), which corresponds to the healthy brain (before the disease). The value of the pressure at the bottom of the phantom (both outside and inside) in this pre-disease stage was 945.7 Pa. Next, the pressure in the cavity was increased to deform the phantom (current configuration), corresponding to the hydrocephalus stage. In this current configuration, which is pre-operative stage in the experiment, the pressure distribution on the outer surface was kept the same as before (945.7 Pa at the bottom of the phantom), while hydrostatic pressure in the rubber membrane was increased, so that the pressure at the bottom of the cavity was 2102.1 Pa. Finally, the "ventriculostomy" was performed by decreasing the internal pressure back to the pre-disease value, and the phantom returned to the intermediate configuration. The 3D CT images were taken both at the intermediate and the current configurations.

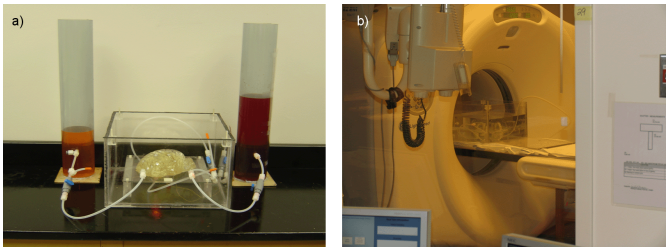

Fig. 2. (a) Experimental setup. (b) Experiments in the CT scanner.

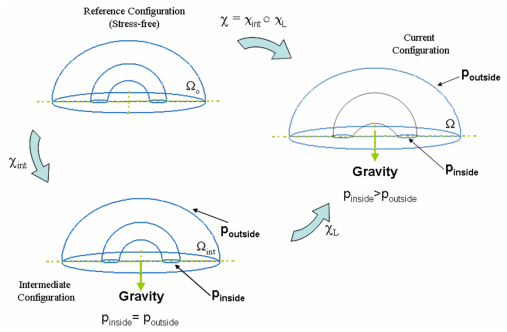

Fig. 3. Schematic kinematics of the experiment.

5 3D Inverse Analysis

Both the phantom and cavity surfaces, before and after the deformation, were extracted from the acquired CT images and meshed using an in-house meshing algorithm (Fig. 4). In order to perform the inverse analysis we need to choose one of the two configurations (Fig. 3) as the initial one. Though it would be more logical to adopt the current (pre-operative) configuration as the initial one, this is not possible, because the stress distribution in the phantom at this pre-operative stage is not known, due to the gradient between the external and internal pressures. In the intermediate (post-operative) configuration, however, the stress distribution is known. The specific gravity (G) of silicone gel is close to unity [19] (Ggel = 0.95), so that silicone phantom is practically suspended in water. Ignoring the difference in densities of gel and water, a series of numerical simulations were performed with ABAQUS. Due to incompressibility of the silicone gel, volume of the phantom does not change. In addition, our simulations showed that all deformations in the silicone phantom are negligible under the hydrostatic boundary loading conditions in the intermediate configuration. That is, the strain level in the intermediate configuration does not exceed 0.5%. Furthermore, the corresponding hydrostatic stress state develops inside the material as it was a liquid of the same specific density. In other words, for all practical purposes, stress response in the body in the intermediate configuration is inde-

pendent of material parameters. Choosing the intermediate configuration as the initial one means that, in reality, we model the disease (hydrocephalus), rather than the operation (ventriculostomy). This however, does not affect the generality of the proposed procedure, due to the reversibility of the disease-operation process in our experiments. Based on these considerations, the meshed surfaces

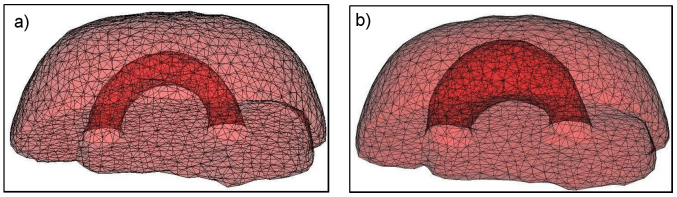

Fig. 4. Surface mesh for (a) non-deformed and (b) deformed phantom.

for the non-deformed phantom (Fig. 4a) were imported into ABAQUS [23] for the Finite Element Analysis. Transferred triangular surface mesh was converted to tetrahedral elements using ABAQUS built-in meshing functions [23]. However in the literature, hexagonal elements are usually a preferred choice for 3D finite element analysis of incompressible materials [10]. It is well known that first-order tetrahedral elements, when modeling incompressible behavior, are susceptible to "mesh locking" [29]. Furthermore, in our simulations using first-order tetrahedral elements, it was not possible to have a converged solution for strains exceeding 10%. Fortunately, modified, second-order tetrahedral elements [23] are available in ABAQUS to provide improved performance over "regular" tetrahedral elements in modeling incompressible materials. These elements are robust during finite deformation and in analyses requiring large element distortions, such as response of rubber components [23]. In particular, in our simulations, using these elements always resulted in convergence even for strains as large as 100%. As a result, since the material is assumed to be incompressible and large element distortions near the inner surface were expected, modified second-order tetrahedron hybrid elements (C3D10MH) were used. Based on the transferred surface mesh, a FEM mesh with 14752 nodes and 9538 elements was generated (Fig. 5c shows a slice of this FE mesh, corresponding to the scanned image slice in Fig. 5a).

A Levenberg-Marquardt based inverse analysis algorithm [24, 25] was linked to ABAQUS to allow for iterative solutions of inverse boundary value problems. The algorithm was first tested on simple geometries (cantilever beam, triaxial compression test, spherical shell expansion, etc) for optimization of parameters of some built-in large strain non-linear elastic models (e.g. Mooney-Rivlin [12], Ogden [14]). The algorithm demonstrated convergence for sufficiently kinematically constrained problems.

The described algorithm was used to optimize the parameter C_{10} of the neo-Hookean material model and the parameters μ_1 and α_1 of the Ogden model (for

$N = 1$) for the 3D finite element model of silicone phantom. For the incompressible case, the neo-Hookean strain energy per unit of reference volume is given by $U = C_{10}(I_1 - 3)$, where C_{10} is a material parameter, I_1 is the first strain invariant, defined as $I_1 = \lambda_1^2 + \lambda_2^2 + \lambda_3^2$, where λ_i are the principle stretches. The Ogden model is given by the strain energy per unit of reference volume, $U = \sum_{n=1}^{N} \frac{\mu_n}{\alpha_n}(\lambda_1^{\alpha_n} + \lambda_2^{\alpha_n} + \lambda_3^{\alpha_n} - 3)$, where μ_1 and α_1 are the material properties.

Boundary conditions were specified as described in the experimental procedures. Then the parameters of the neo-Hookean and Ogden models were determined by minimizing the mean square deviations between the calculated (Fig. 5d) and observed (Fig. 5b) displacements [1]. The calculated parameter value for the neo-Hookean model was $C_{10} = 663.7\ Pa$, which falls well within the range of the corresponding parameter values given in the literature (Table 1). Stiffness of silicone gel can be controlled by catalyst and resin ratio of the mixture, i.e. increasing the resin proportion increases the gel stiffness. This explains the large difference of the calculated parameter C_{10} between this study and Dokos et al. [26] as well as Augenstein et al. [27] since in their study catalyst-to-resin ratio is twice greater than ours (Table 1). In Rajagopal et al. [21] and Chung et al. [28], there is no information about curing conditions of the gels tested. In our laboratory, we observed that time and temperature of curing have strong effect on the stiffness of the silicone gel. In addition to different catalyst-to-resin ratio, one possible explanation for the difference in our C_{10} and that obtained by Rajagopal et al. [21] and Chung et al. [28] may be the curing conditions.

In order to demonstrate the reliability of IGCM, we also derived the material properties of the silicone gel via independent tests without using any image guidance technique. For this purpose, a cylindrical sample with diameter and height of 82 mm was prepared using the same conditions as described in Sec. 3 and tested in uniaxial compression with no-slip boundary conditions. The experiment was performed in water to minimize the effect of gravity on measurements as discussed above. The no-slip boundary conditions were created by attaching coarse sandpaper to the faces of loading plates. The displacement of the sample boundaries versus the applied axial load were measured during the experiment. Although, analytical solution of this problem is available, it still requires a numerical solution of a system of transcendental algebraic equations [31]. This is why to determine the material parameter C_{10}, the experiment was simulated directly in ABAQUS using the neo-Hookean model. The 8-node biquadratic hybrid reduced integration (CAX8RH) elements were used in the simulations. This type of element works well for axisymmetric finite element modeling of large deformations of incompressible materials [23]. The numerical solution was fitted to the test data using the least-squares method (Table 1). Material parameters of the silicone gel, derived from IGCM and independent uniaxial compression test, differ by 20% from each other. A similar magnitude of deviation is observed by Dokos et al. [26]. They performed 3 different tests (tensile, rotational shear and simple shear tests) on silicone gel and their tensile and simple shear test results also showed approximately 20% difference. Such magnitude of deviation is also

typical for experiments with rubber compounds [26, 30]. As a result, we conclude that the material parameters calculated by IGCM and uniaxial compression test agree reasonably well. Note that using lubricated sample ends (slip boundary conditions) would be much easier for interpretation of the test results since this case is truly 1D and does not require any numerical simulation. However, even a small uncertainty in shear tractions at the sample ends may considerably affect the test results [32]. Therefore, we decided to use the no-slip boundary condition which makes the test interpretation more complex, but eliminates any uncertainty. The calculated parameter values for Ogden model were $\mu_1 = 1332.1\ Pa$

$\mathbf{C_{10}}$[kPa]	Reference	Catalyst-to-Resin Ratio
8.99-13.31	Dokos et al. [26]	1:2
8.72-9.91	Augenstein et al. [27]	1:2
0.426	Chung et al. [28]	N/A
3.11	Rajagopal et al. [21]	N/A
0.6637	This study (IGCM)	1:1
0.8466	This study (uniaxial compression)	1:1

Table 1. Parameter values of neo-Hookean model for the silicon gel.

and $\alpha_1 = 1.9819$. These values are consistent with those of the neo-Hookean model (note, that for $\alpha_1 = 2$ and $\mu = 2C_{10}$ the two models are equivalent). This confirms that the neo-Hookean model is a reasonable assumption for modeling the silicon gel behavior, and at the same time demonstrates that the utilized inverse analysis algorithm is also capable of handling two parameter non-linear models successfully.

6 Conclusions

The IGCM was performed in the controlled environment: on the silicone brain phantoms closely simulating the in-vivo brain geometry, mechanical properties and boundary conditions. The ventriculostomy was simulated by consequently inflating and deflating the internal rubber membrane. The obtained images were analyzed to derive displacement fields, meshed, and incorporated into ABAQUS. The subsequent Inverse Finite Element Analysis allowed for optimization of the parameters of the neo-Hookean and Ogden elastic models for the phantom material. The calculated mechanical properties were consistent with those in the literature and those obtained from the independent uniaxial compression tests, providing preliminary justification for the future application of the IGCM to in-vivo brain tissue, which has a number of clinical applications.

Acknowledgments. The authors are grateful to Prof. J. A. Fountain, Dept. of Radiology, Emory University, for his help with the CT imaging. This research was partly supported by the NIH under grants EB02957 and LM08128.

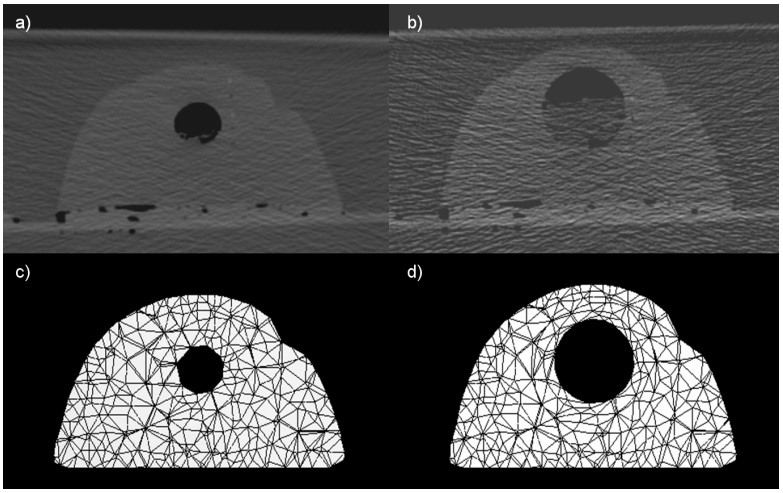

Fig. 5. A scanned image slice (a) before and (b) after the deformation. The corresponding slices of the finite element meshes are shown in c) and d), respectively.

References

1. Puzrin, A., Skrinjar, O., Ozan, C., Kim, S. and Mukundan, S. "Image guided constitutive modeling of the silicone brain phantom", *SPIE Medical Imaging*, San Diego, CA, 2005.
2. Fung, Y.C. Biomechanics. Mechanical properties of living tissues. Springer, New York, 1981.
3. Fallenstein, G.T., and Hulace, V.D. "Dynamic mechanical properties of human brain tissue.", *Journal of Biomechanics*, 2:217-226, 1969.
4. Metz, H., McElhaney, J.H., and Ommaya, A.K. "A comparison of the elasticity of live, dead, and fixed brain tissue.", *Journal of Biomechanics*, 3:453-458, 1970.
5. Pamidi, M.R. and Advani S.H. "Nonlinear constitutive relations for human brain tissue.", *Journal of Biomechanical Engineering*, 100:44-48, 1978.
6. Mooney, M. "A theory of large elastic deformation.", *J. of Applied Physics*, 11:582-592, 1940.
7. Walsh, E.K., and Schettini, A. "Calculation of brain elastic parameters in vivo.", *American Journal of Physiology*, 247:637-700, 1984.
8. Sahay, K.B., Mehrotra, R.,Schdeva, U., and Banerji, A.K. "Elastomechanical characterization of brain tissues.", *Journal of Biomechanics*, 25(3):319-326, 1992.
9. Hart-Smith, L.J. "Elasticity parameters for finite deformation of rubber-like materials.", *Z. angew. Math. Phys.*, 17:608-626, 1966.
10. Mendis, K.K., Stalnaker, R. L., and Advani, S.H. "A constitutive relationship for large deformation finite element modeling of brain tissue.", *Trans. ASME Journal of Biomedical Engineering*, 117:279-285. 1995.
11. Miller, K., Chinzei, K., Orssengo, G. and Bednarz, P. "Mechanical properties of brain tissue in-vivo: experiment and computer simulation.", *Journal of Biomechanics*, 33:1369-1376, 2000.
12. Rivlin, R.S. "Forty years of nonlinear continuum mechanics.", *IX International Congress on Rheology*, Mexico, 1-29, 1984.

13. Miller, K. and Chinzei, K. "Mechanical properties of brain tissue in tension.", *Journal of Biomechanics*, 35: 483-490, 2002.
14. Ogden, R.W. "Large deformation isotropic elasticity - on the correlation of theory and experiment for incompressible rubberlike solids.",*Royal Society London Series A*, 326:565-584, 1972.
15. Bradshaw, D. R. S. et al.. "Simulation of acute subdural hematoma and diffuse axonal injusry in coronal head impact.", *Journal of Biomechanics*, 34(1):85-94, 2001.
16. Ivarsson, J. et al.. "Strain relief from the cerebral ventricles during head impact: experimental studies on natural protection of the brain.", *Journal of Biomechanics*, 33(2):181-189, 2000.
17. Audette, M. A. et al.. "Level-Set Surface Segmentation and Fast Cortical Range Image Tracking for Computing Intrasurgical Deformations.", *Medical Image Computing and Computer-Assisted Intervention (MICCAI)*, Cambridge, UK, 788-797, 1999.
18. Brands, D.W.A., Bovendeerd, P.H.M., van Campen, D.H., Wismans, J.S.H.M., and van Bree, J.L.M.J. "Silicon Gel, a Mechanical Brain Tissue Model.", *Proc. Stapp Car Crash Conference*, 1999.
19. Dow Corning. Information about Dow Corning brand dielectric gels. Dow Corning Corporation, Midland, Michigan 48686-0994, 2002.
20. Azar, F.S., Metaxas, D.N., Miller, R. T. and Schall, M.D. "Methods for Predicting Mechanical Deformations in the Breast during Clinical Breast Biopsy.", *IEEE 26th Annual Northeast Bioengineering Conference*, 2000.
21. Rajagopal, V, Nielsen , P.M.F and Nash, M.P. "Development of a three-dimensional finite element model of breast mechanics", *26th Annual International Conference of the IEEE EMBS*, San Francisco, CA, Sept. 1-5, 5080-5083, 2004.
22. Holzapfel G.A. Nonlinear Solid Mechanics. A continuum approach for engineering, John Wiley and Sons, England, 2000.
23. ABAQUS ®. Version 6.5-4, User's Manual and Theory Manual. Hibbit, Karlson and Sorensen, Inc, 2004.
24. Levenberg, K. "A method for the solution of certain non-linear problems in least squares", *Quart. Appl. Math.*, 2:164-168, 1944.
25. Marquadt, D.W. "An Algorithm for Least-Squares Estimation of Nonlinear Parameters", *Journal of the Society for Industrial and Applied Mechanics*, 11(2): 431-441, 1963.
26. Dokos, S, Legrice, I. J., Smaill, B. H, Kar, J and Young, A. A. "A triaxial-Measurement Shear-test device for soft biological tissues", *Journal of Biomechanical Engineering*, 122:471-478, 2000.
27. Augenstein K. F., Cowan B.R., Legrice, I.J., Nielsen, P.M.F. and Young A.A. "Method and Apparatus for soft tissue material parameter estimation using tissue tagged magnetic resonance imaging", *Journal of Biomechanical Engineering*, 127:148-157, 2005.
28. Chung, J., Rajagopal, V, Nielsen , P.M.F and Nash, M.P. "Computational modeling of the breast during mammography for tumor tracking", *Proceedings of SPIE MI 2005*, 5746, 817-824, 2005.
29. Bathe, K.J. Finite element procedures. Prentice Hall, 1996.
30. Raos, P, "Modelling of Elastic Behavior of Rubber and Its Application in FEA", *Plastics, Rubber Compos. Proc. Appl.*, 19:293-303., 1993.
31. Klingbeil, W.W., Shield, R.T. "Large-deformation analyses of bonded elastic mounts", Z.A.M.P., 17(20):281-305, 1966.
32. Miller, K. "Method of testing very soft biological tissue in compression", *Journal of Biomechanics*, 38:153-158, 2005.